BULLETIN OF THE POLISH ACADEMY OF SCIENCES
TECHNICAL SCIENCES, Vol. 69(5), 2021, Article number: e137942
DOI: 10.24425/bpasts.2021.137942

Multi-sourced power system restoration strategy based on modified Prim's algorithm

Artur ŁUKASZEWSKI and Łukasz NOGAL *

Electrical Power Engineering Institute, Faculty of Electrical Engineering, Warsaw University of Technology,
ul. Koszykowa 75, 00-662 Warsaw, Poland

Abstract. Self-healing grids are one of the most developing concepts applied in electrical engineering. Each restoration strategy requires advanced algorithms responsible for the creation of local power systems. Multi-agent automation solutions dedicated for smart grids are mostly based on Prim's algorithm. Graph theory in that field also leaves many problems unsolved. This paper is focused on a variation of Prim's algorithm utility for a multi-sourced power system topology. The logic described in the paper is a novel concept combined with a proposal of a multi-parametrized weight calculation formula representing transmission features of energy delivered to loads present in a considered grid. The weight is expressed as the combination of three elements: real power, reactive power, and real power losses. The proposal of a novel algorithm was verified in a simulation model of a power system. The new restoration logic was compared with the proposal of the strategy presented in other recently published articles. The novel concept of restoration strategy dedicated to multi-sourced power systems was verified positively by simulations. The proposed solution proved its usefulness and applicability.

Key words: self-healing grid; micro-grid; reconfiguration; greedy algorithms; graph theory; simulations; Prim's algorithm.

NOMENCLATURE

Symbols

α^j	j-th power source capacity coefficient
b_1	Minimum real power in set $\{P_{PS0}+P_k\}$
b_2	Minimum reactive power in a set $\{\lvert Q_{PS0}+Q_k\rvert\}$
c_1	Minimum real power in set $\{P_{PS0}+P_k\}$
c_2	Minimum reactive power in a set $\{\lvert Q_{PS0}+\Delta Q_k+Q_k\rvert\}$
c_3	Minimum real power loss in set $\{\Delta Q_k\}$
I_{MAX}	Maximum value of generator stator current
k	Edge/transmission line number for which weight is calculated
i	Number of edges which can be connected to a grid topology and do not create cycle subgraphs in a topology
j	Power source number for which weight and a capacity factor are calculated
$\{\ldots\}$	Set of calculated power grid consecutive parameters for T_k, set contains i elements
p	Impact coefficient of total real and total reactive power of calculated weight of an edge
E_q	$q-$axis component of the steady-state internal electromotive force proportional to the field winding self-flux linkages
δ_{MAX}	Maximal power angle of synchronous generator guaranteeing its stability
x_d	total d-axis synchronous reactance between a generator and an infinite busbar
V	Output voltage of a synchronous generator
$P_{G\min}$	Minimal power generated by a turbine
$P_{G\max}$	Maximal power generated by a turbine
S	Total apparent power output of a synchronous generator
n^j	Effective number of all possible to connection lines (edges)
n^j_{all}	Number of all possible to connection lines (edges)
n^j_{cycles}	Number of all possible to connection lines (edges) creating cycle graphs in a considered topology
P	Total real power output of a synchronous generator
Q	Total reactive power output of a synchronous generator
w_k	Weight calculated for k-th graph edge for T_k
w^k_1	Weight element bounded with real power, with not included losses, calculated for k-th graph edge for T_k
w^k_2	Weight element bounded with reactive power, with not included losses, calculated for k-th graph edge for T_k
w^{*k}_1	Weight element bounded with real power, with not included losses, calculated for k-th graph edge for T_k
w^{*k}_2	Weight element bounded with reactive power, with included losses, calculated for k-th graph edge for T_k
w^{*k}_3	Weight element bounded with real power losses calculated for k-th graph edge for T_k
P_k	Real power at the receiving end of k-th transmission line
P_r	Total real power delivered by sources to micro-grids (the result of simulation)
P_s	Rated real power output of a source
P^j_s	Rated real power output of j-th source
P_{PS0}	Total real power of topology T_0
P^j_{PS0}	Total real power of topology T^j_0
P^j_{PSk}	Total real power of topology T^j_k

*e-mail: lukasz.nogal@pw.edu.pl

Manuscript submitted 2021-04-13, revised 2021-06-02, initially accepted for publication 2021-06-24, published in October 2021

Q_r	Total reactive power delivered by sources to micro-grids (the result of simulation)
Q_k	Reactive power at the receiving end of k-th transmission line
Q_{PS0}	Total reactive power of topology T_0
Q^j_{PS0}	Total reactive power of topology T^j_0
Q^j_{PSk}	Total reactive power of topology T^j_k
ΔP_r	Total real power losses in the created micro-grids (the result of simulation)
ΔP_k	Total real power losses of topology T_k
ΔP^j_k	Total real power losses of topology T^j_k
P_L	Real power sum of all loads present in the considered grid
ΔQ_k	Total reactive power losses of topology T_k
ΔQ^j_k	Total reactive power losses of topology T^j_k
S_r	Total apparent power delivered by sources to micro-grids (the result of simulation)
p_1	Impact coefficient of real power on weight
p_2	Impact coefficient of reactive power on weight
p_3	Impact coefficient of real power losses on weight
T_0	Power grid topology considered before connection of k-th transmission line for a single source power system
T^j_0	Topology considered before connection of k-th transmission line to a microgrid created for j-th source
T_k	Power grid topology considered after connection of k-th transmission line for a single source power system
T^j_k	Topology considered after connection of k-th transmission line to a micro-grid created for j-th source
MLR	Maximum load restoration
$MRPL$	Minimum real power loss of restored power grid
$\boldsymbol{C}$	Adjacency matrix/matrix topology of connected transmission lines being the result of a program based on Prim's algorithm
$\boldsymbol{I}$	Adjacency matrix of transmission lines rated currents
$\boldsymbol{V}^j_k$	Voltage nodal matrix for considered topology T^j_k
$\boldsymbol{W}$	Adjacency matrix of weights for lines which can be connected to the topology T^j_0 and do not lead to the creation of a cycle subgraph in the structure
$\boldsymbol{Z}$	Impedance matrix of a power grid
$\boldsymbol{Z}^j_k$	Impedance matrix of power grid for considered topology T^j_k
$\boldsymbol{I}^j_k$	Adjacency matrix of the currents transmitted by the lines for the considered topology T^j_k
$\boldsymbol{P}$	Adjacency matrix of real power loads connected to grid nodes
$\boldsymbol{Q}$	Adjacency matrix of reactive power loads connected to grid nodes
$\boldsymbol{P}^j_W$	Adjacency matrix of transmission lines which contains computed P^j_{PSk} powers
$\boldsymbol{Q}^j_W$	Adjacency matrix of transmission lines which contains computed Q^j_{PSk} powers
$\boldsymbol{P}^j_k$	Adjacency matrix of real power loads connected to j-th source for a grid represented by topology T^j_k
$\boldsymbol{Q}^j_k$	Adjacency matrix of reactive power loads connected to j-th source for a grid represented by topology T^j_k
$\boldsymbol{J}$	Matrix of all j indexes of power sources in the considered grid
$\boldsymbol{J}^*$	Matrix containing j indexes of power sources, being the result of algorithm calculations
$\boldsymbol{J}^{**}$	Matrix containing j indexes of power sources which have a minimal value of n^j factor
α	Matrix of calculated α^j factors
$\boldsymbol{C}_L$	Matrix of connected loads
t	Simulation time

Abbreviations

BBT	Busbar connected to a transformer
G	Generator
L	Transmission line
PS	Power system
T	Transformer

1. INTRODUCTION

The expectation of reliability in power delivery leads to the development of smart grid technologies [1]. Reliability requires hardware coordination with control algorithms [2].

In computer sciences, various algorithms are available which can be used for a power system restoration or reconfiguration strategy due to grid failure [1–12]. A lot of popular solutions are based on Prim's algorithm [11].

Various strategies using graph theory are available. Some of them are bounded with real power [13]. The control code simplicity is the main advantage of this methodology [14]. Unfortunately, the control logic based only on one parameter makes it impossible to create the power grid configuration flexibly. An additional disadvantage of logic using the Prime algorithm is the way of creating topology for individual sources supplying consumers [15]. This topology results in the configuration of the power system without supplying all loads. In other cases, the use of graph theory comes down to the topology sectioning method [16]. Such solutions use the assignment of weighting factors to individual power lines, depending on active and reactive power. High flexibility in shaping the obtained grid configuration is the advantage of this approach. However, the high complexity of the algorithm is the disadvantage of this solution. It is so because in the first step logic cuts the power system graph into smaller micro-grids where each one is supplied with an independent energy source. Then, in the second stage, Prim's algorithm is used to create connections of the transmission lines [7]. The advanced algorithm also affects the time of its implementation by the microprocessor system significantly [13].

All the above-mentioned issues remain open problems and this paper focuses on the suggestions which can be instrumental in graph theory applications in power system restoration strategies. Therefore, a new algorithm idea is presented in the paper. For our purposes, weights have been multi-parametrized and combine real power, reactive power and power losses. The proposed solution is embedded in the modified Prime's algorithm, which is dedicated to system structure sourced by a few energy generators. Our original solution has been verified in simulation calculations.

It was necessary to use reference logic to check the proposed algorithm. After the analysis, the logic from the article [11] was considered as the comparative algorithm. This decision resulted directly from the fact that the solution in [11] combines the advantages of other published control logics from [1–10].

2. PROBLEM FORMULATION

In [12], the multi-power source system structure is partitioned by special algorithms because Prim's algorithm is dedicated to single-source topologies. This kind of strategy consists of three stages. The first one is called coarsening phase, the second one is the initial partitioning phase, and the last one is referred to as an uncoarsening and refinement phase. In the first stage, graph G_0 is transformed into groups of smaller structures G_1, G_2, …, G_k. In the second phase, part P_k of the coarsest graph G_k minimizes the set of edges and weight constraints are calculated. Graph partitioning may be proceeded for instance by a recursive bisection algorithm. In the last stage, the partition P_k brings the model back to the starting structure G_0 through graphs G_{k-1}, G_{k-2}, …, G_1, G_0. The whole process is based on graph edge representation as a "weight" [17]. Figure 2 shows the example of the idea of graph partitioning and Fig. 3 presents a power system structure after partitioning. Weights are yet another important problem in the accommodation of graph theory to power system models used in the Smart Grid restoration strategies [18].

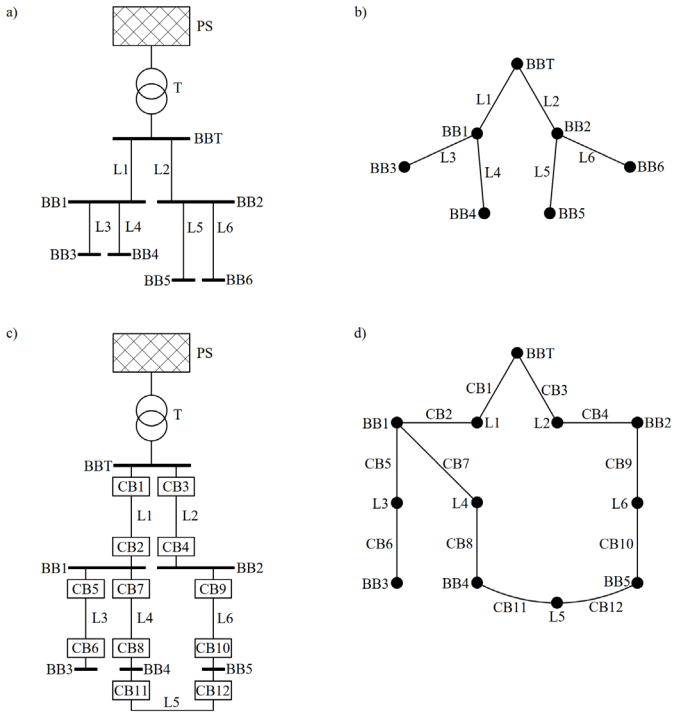

Fig. 1. Power system representation as a graph structure; a) power system model with transmission lines (L) and busbars (BB); b) graph structure for a grid from a); c) power system model with transmission lines (L), circuit breakers (CB), and busbars (BB); d) graph structure for a grid from c)

Weights may have static or variable values [19]. Variable values are proper for a power system because of the presence of losses and reactive power in a distribution grid [20]. Based on the idea of presenting the power system in Figs. 1a and 1b, the methodology of weights calculation combined with Prim's algorithm for a power system is explained in Fig. 4. The topology in the first stage is marked in red color. In the next step, Prim's

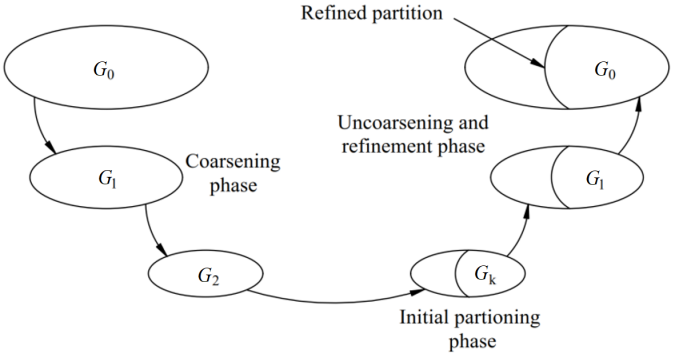

Fig. 2. Graph partitioning process

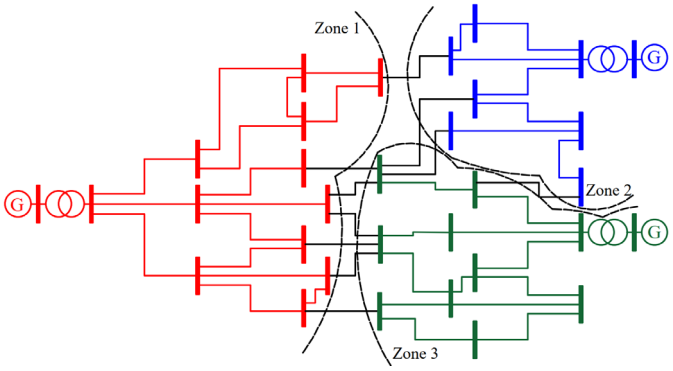

Fig. 3. Example of micro-grids created in the power system partitioning process

algorithm has to decide which of the lines expressed mathematically by weights, marked in green, is the optimal one and is going to be added to the red structure in the next step [12]. Before the edge is chosen, it is necessary to calculate the needed weights [10]. Those parameters have to be computed for green lines (L3, L4, L5, L6).

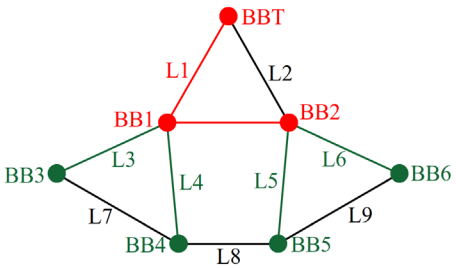

Fig. 4. Example of graph: powered in the beginning structure (red), edges not connected, which weights have to calculated for a Prim's algorithm (green), and non-transmitting current lines (black)

Weights should be represented by mathematical formulas as simple as possible as it influences calculation efficiency [21]. The expression used for weights calculation has to include the presence of such parameters as real power and reactive power [22] in a power system. It is problematic because these variables are components of a complex number that graphically is identified as a phasor [23]. Some authors have made a simplification and suggested weights calculation based solely on

a single parameter [11]: real power. Weights, in this case, are expressed by the following equation:

$$w_k = \frac{P_{PS0} + P_k + \Delta P_k}{P_s}. \tag{1}$$

A different idea was included in [12]. In this case, weights of edges are represented by a much more complicated mathematical formula [12]:

$$w_k = \frac{w_1^k}{b_1} \cdot p + \frac{w_2^k}{b_2} \cdot (1-p). \tag{2}$$

Parameters w_1^k and w_2^k are expressed by the following equations [7]:

$$w_1^k = P_{PS0} + P_k, \tag{3}$$

$$w_2^k = |Q_{PS0} + Q_k|. \tag{4}$$

Factors b_1 and b_2 are equal [7]:

$$b_1 = \min(P_{PS0} + P_k), \tag{5}$$

$$b_2 = \min|Q_{PS0} + Q_k|. \tag{6}$$

The last parameter present in equation (2) is coefficient p, which can be also called the preference factor. This variable represents a correlation between real power and reactive power.

Still evolving concepts of a self-healing grid require further improvements of algorithms responsible for power system restoration strategies [24]. All of the solutions mentioned above are imperfect. It is important to adapt the most popular Prim's algorithm for multi-sourced power system structure [25]. This kind of modification allows for a much more efficient calculation process in comparison to logics based on graph partitioning in which weights are calculated twice [26]. The first time they are required to split the graph structure to subgraphs and the second time they are used to create lines connection in micro-grids [27].

The next problem is connected with weights. It is crucial to include power losses influence in their equations. Single variable formula (1) is simple, but it does not guarantee optimal connections for AC-current grids because stability is also dependent on reactive power. Equation (2) is much more flexible, but it also skips power losses.

Consequently, all of the problems discussed here should be addressed and solved adequately. This is what we have set out to do in this paper by proposing the novel concept of weight calculation formula and modified restoration algorithm for a multi-sourced power system.

3. CONTRIBUTION

This paper includes a proposal of a new mathematical formula with power losses influence factor which can be used to calculate edge weights for a graph power system representation. A concept of modified Prim's algorithm dedicated to multi-sourced structures is another important contribution. All the presented ideas have been successfully verified in a simulation model and their utility was confirmed in comparison with the algorithm described in [11].

An algorithm verification process was based on the following assumptions on the following objectives:

- maximum load restoration:

$$MLR = \frac{P_r - \Delta P_r}{P_L}, \tag{7}$$

- minimum real power loss of restored power grid:

$$MRPL = \frac{\Delta P_r}{MLR}. \tag{8}$$

Equation (8) is used as a second sub-algorithm verification condition when the same *MLR* values for more than one connection topology are achieved. In such a situation, optimal topology is defined by equation (8) for a structure with the lowest value of that factor.

4. RESTORATION ALGORITHM DEDICATED FOR MULTI-SOURCED MICRO-GRIDS

It has to be possible to apply the algorithm in the context of micro-grids whose structures include more than one energy source [28]. Such a logic requires the implementation of many additional conditions such as power system voltage limits, current limits in transmission lines and power source capability inequations, etc. [29].

4.1. Power source capability

Power energy sources have a specific real and reactive power capability [30]. Limits are expressed by mathematical formulas [31]. The following inequations [32] are the most popular inequations used for instance for classical power plants:

$$P^2 + Q^2 = S^2 \leq (VI_{\mathrm{MAX}})^2, \tag{9}$$

$$P^2 + \left(Q + \frac{V^2}{x_d}\right)^2 \leq \left(\frac{E_q V}{x_d}\right)^2, \tag{10}$$

$$P \geq \left(Q + \frac{V^2}{x_d}\right) \cdot \tan\delta_{\mathrm{MAX}}, \tag{11}$$

$$12 P_{G\min} \leq P \leq P_{G\max}. \tag{12}$$

4.2. Busbar voltage and transmission line current limits

The restoration algorithm has a section which calculates edge weights. This value is dependent on two conditions. The first one is a limit of busbar voltage, the second one is the maximal current possible to be transmitted by line.

Voltage limits and power system test models are presented in many publications. In IEEE benchmarks, the limit is the set ranging from 0.9 pu to 1.1 pu [33]. Different conditions are defined in [12] and it is a limit from 0.95 pu to 1.05 pu. Permitted voltages for busbars should be set specifically for a considered micro-grid structure [34].

Transmission lines may be in the ground or in the air as their placement influences the maximal current [35]. This value cannot be exceeded and this condition must be implemented in sub-algorithm responsible for weights computation.

4.3. Novel concept of weight calculation formula

The procedure of weights calculation is at the core of the methodology of greedy algorithms. The idea presented in this paper is based on a modification of equation (2).

In a power system, distribution losses are present. Equation (2) does not include them. The following concept of weight is much more representative:

$$w_k = \frac{w_1^{*k}}{c_1} \cdot p_1 + \frac{w_2^{*k}}{c_2} \cdot p_2 + \frac{w_3^{*k}}{c_3} \cdot p_3 \,. \tag{13}$$

Parameters w_1^{*k} are expressed by equation (5), but to compute the w_2^{*k} and w_3^{*k} correctly the following equations need to be applied:

$$w_1^{*k} = P_{PS0} + P_k \,, \tag{14}$$

$$w_2^{*k} = |Q_{PS0} + Q_k + \Delta Q_k| \,, \tag{15}$$

$$w_3^{*k} = \Delta P_k \,. \tag{16}$$

Factors c_1, c_2 and c_3 are equal:

$$c_1 = \min\left(P_{PS0} + P_k\right), \tag{17}$$

$$c_2 = \min|Q_{PS0} + Q_k + \Delta Q_k| \,, \tag{18}$$

$$c_3 = \min \Delta P_k \,. \tag{19}$$

Consideration of weight as a sum of real power loads by equation (2) is misleading. Let us analyze the structure shown in Fig. 5. In this example, an assumption is made that reactive power is not included and a DC grid is the analyzed system. The decision as to which transmission line should be connected is made by Prim's algorithm. Source limit is equal to 1.5 p.u. and does not allow to energize all busbars. For equation (2), when factor $p = 1$, line L1 and L2 weights are equal to 1.0 and 1.4, respectively. In the case when the weight is computed by equation (13) and factors $p_1 = p_2 = p_3 = 1$, the results are completely different. The weights for lines L1 and L2 are equal to 3.0 and 2.4, respectively. Prim's algorithm with implemented equation (2) would choose to connect line L1, but for equation (13) that would be line L2. From the point of view of economy, it is more optimal to energize loads with the higher value. In the example shown in Fig. 5, applying the definition of optimality Prim's algorithm is expected to connect busbar BB2 to PS. The presented example proves the utility of equation (13).

Optimality for p_1, p_2 and p_3 has to be identified for a defined group of conditions. In this case, an approach based on particle swarm optimization (PSO) is useful. The optimization method uses conditions based on equations (7) and (8). The most optimal solution is in the case when all loads are energized and the real power loss in created topology has the lowest value. It happens when *MLR* factor is equal to 1 and *MRLP* has the lowest value for an analyzed set of the p_1, p_2 and p_3 factors.

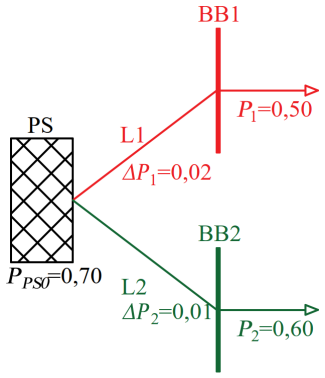

Fig. 5. Example of power system with optimal connected line (green color) when weight is calculated by formula (11), and suboptimal behavior of Prim's algorithm for equation (2)

4.4. Novel concept of conditions determining loads connection order to the power sources

Prim's algorithm dedicated to a multisource power system topology requires logic responsible for switching between micro-grids created for each of energy generators. Consistency without such a balance can lead to suboptimal transmission line connections. In this case, not optimal behavior is defined as an algorithm result given as a grid structure when in the beginning stages one or more power sources are separated and the left feeders cannot supply the rest of the loads. Figure 6 is an example of such a topology when switching between sources was made in a set order one-by-one. The steps in which transmission lines have been connected are in round brackets.

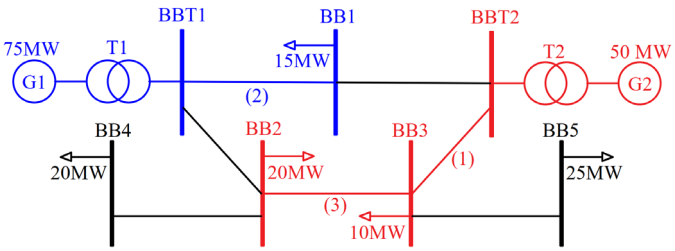

Fig. 6. Example of power system with suboptimal transmission line connections (blue color for G1 and red color for G2)

The situation in Fig. 6 may be avoided when the decision is made as to which feeder the new load should be connected, after analyzing the proper conditions. The first of the proposed requirements is specified by the following formula:

$$n^j = n^j_{all} - n^j_{cycle} \,. \tag{20}$$

Equation (20) calculated for every source in the considered topology sets the priority to the feeder with the lowest n^j-coefficient, representing the number of transmission line connection attempts which in the graph model do not create cycles. Figure 7 shows in a graphical form the explanation why such an approach is correct When the primary goal is to connect lines first to a source with a higher value of the specified factor (20), the resulting topology does not supply all loads. The power of the G2 source is insufficient to include the additional load on

the BB4 bus. The situation is completely different in the case when the power supply is realized based on the lowest value of the factor n^j. In this case, we can talk about the optimal operation of the algorithm because all the loads have been powered. The steps in which transmission lines in each case have been connected are in round brackets.

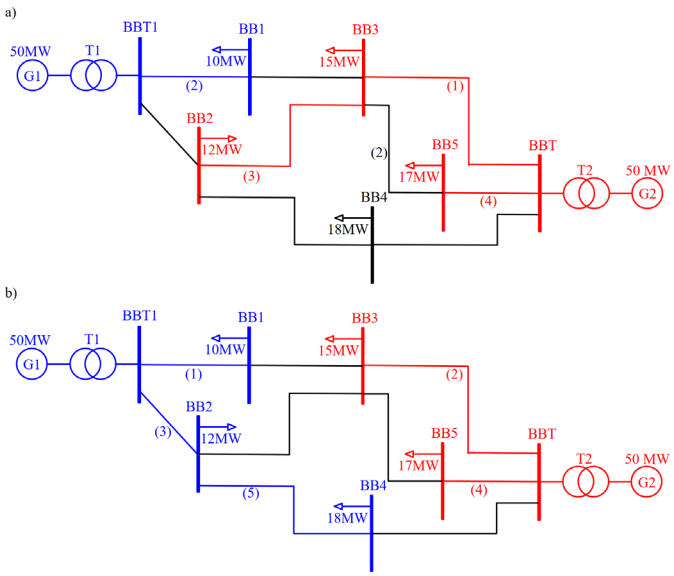

Fig. 7. Example of power system restoration process with a) suboptimal transmission line topology when connection priority was defined for source characterized by maximal n_j coefficient and b) optimal transmission line topology when connection priority was defined for source characterized by minimal n_j coefficient

The second of defined requirements is connected with power source capacity which changes with every connected transmission line. It is expressed mathematically by:

$$\alpha^j = P_s^j - P_{PS0}^j. \tag{21}$$

This requirement is useful in a situation when the conditions implicated by equation (20) are not unequivocal. This is the case when at least for two sources the computed n^j factors have the same values.

4.5. Algorithm structure

The algorithm operates on matrices representing power system structure. The following static arrays with constant dimensions are required: $\boldsymbol{C}$, $\boldsymbol{I}$, $\boldsymbol{J}$, $\boldsymbol{P}$, $\boldsymbol{Q}$, $\boldsymbol{W}$ and $\boldsymbol{Z}$. Additionally, during the computation process, the algorithm creates matrices with dimensions dependent on the structure of the analyzed grid.: $\boldsymbol{I}_k^j$, $\boldsymbol{J}^*, \boldsymbol{J}^{**}, \boldsymbol{P}_k^j, \boldsymbol{P}_W^j, \boldsymbol{Q}_k^j, \boldsymbol{Q}_W^j, \boldsymbol{V}_k^j, \boldsymbol{Z}_k^j, \boldsymbol{C}_L$ and α belong to that group. Calculation logic starts the micro-grid restoration process when all transmission lines have open circuit breakers. At the initialization of the algorithm, k parameter equals 1 ($k = 1$).

The algorithm responsible for spanning tree computation for multi-sourced grid has the following structure:

1. Compare α^j coefficients for sources $\left(j = 1, \ldots, i^j\right)$ and create a set of the j-indexes for which α^j has a maximal value. Then go to step 2.
2. Start weight calculation for the j-th source, where j is equal to the first term in the computed set in step 1 and go to step 3. Weights are calculated for edges that after connection do not create cycles in topology and do not create energy transfers between micro-grids.
3. Compute the following parameters for topology when connecting the k-th line to the j-th source is considered: ΔP_k^j, ΔQ_k^j, $\boldsymbol{I}_k^j$ and $\boldsymbol{V}_k^j$. This process requires the creation of the $\boldsymbol{P}_k^j$, $\boldsymbol{Q}_k^j$ and $\boldsymbol{Z}_k^i$ matrices. Computation can be proceeded by i.e., Newton–Rhapson method. After the completion of the calculation process, go to step 4.
4. Verify the following: is the voltage at all busbars for the k-th transmission line in the analyzed topology within the predefined limits? In this case, the range is set from 0.95 pu to 1.05 pu.
   (a) If YES, go to step 5.
   (b) If No, go to step 13.
5. Are all terms in the $\boldsymbol{I}_k^j$ matrix within the rated ranges when the k-th transmission line is connected?
   (a) If YES, go to step 6.
   (b) If No, go to step 13.
6. Compute total powers delivered by j-th power source when k-th line is energized. At this end, the following formulas are used:

$$P_{PSk}^j = P_{PS0}^j + P_k + \Delta P_k, \tag{22}$$

$$Q_{PSk}^j = Q_{PS0}^j + Q_k + \Delta Q_k. \tag{23}$$

7. Are P_{PSk}^j and Q_{PSk}^j in operational limits for j-th source energizing k-th transmission line in considered topology?
   (a) If YES, go to step 8.
   (b) If No, go to step 13.
8. Put P_{PSk}^j and Q_{PSk}^j into $\boldsymbol{P}_W^j$ and $\boldsymbol{Q}_W^j$ matrices and go to step 9.
9. Is $k := i$?
   (a) If YES, go to step 11.
   (b) If No, go to step 10.
10. Update k value by the formula:

$$k := k + 1 \tag{24}$$

and go to step 3.
11. Update k value by the formula:

$$k := 1 \tag{25}$$

and go to step 12.
12. Are all terms in $\boldsymbol{P}_W^j$ singular values?
   (a) If YES, go to step 14.
   (b) If No, go to step 20.
13. Update P_{PSk}^j and Q_{PSk}^j values into:

$$P_{PSk}^j := -1, \tag{26}$$

$$Q_{PSk}^j := 0. \tag{27}$$

14. Calculate c_1, c_2 and c_3 by equations (17), (18) and (19). Then go to step 15.

15. Is the term for k-th transmission line in $\boldsymbol{P}_W^j$ a positive number?
    (a) If YES, go to step 16.
    (b) If No, go to step 19.
16. Compute weight w_k by equation (13) and set this value into $\boldsymbol{W}$ matrix. Then go to step 17.
17. Is $k := i$?
    (a) If YES, go to step 21.
    (b) If No, go to step 18.
18. Update k value following equation (24) and go to step 15.
19. Set weight $w_k :=$ for the k-th considered transmission line and go to step 17.
20. Put the considered j-th source index into $\boldsymbol{J}^*$ matrix and go to step 23.
21. Are all calculated weights singular values in $\boldsymbol{W}$ matrix?
    (a) If YES, go to step 20.
    (b) If No, go to step 22.
22. Connect to j-th source (source for which weights were calculated) edge with the lowest weight and update $\boldsymbol{C}$ matrix. Then go to step 24.

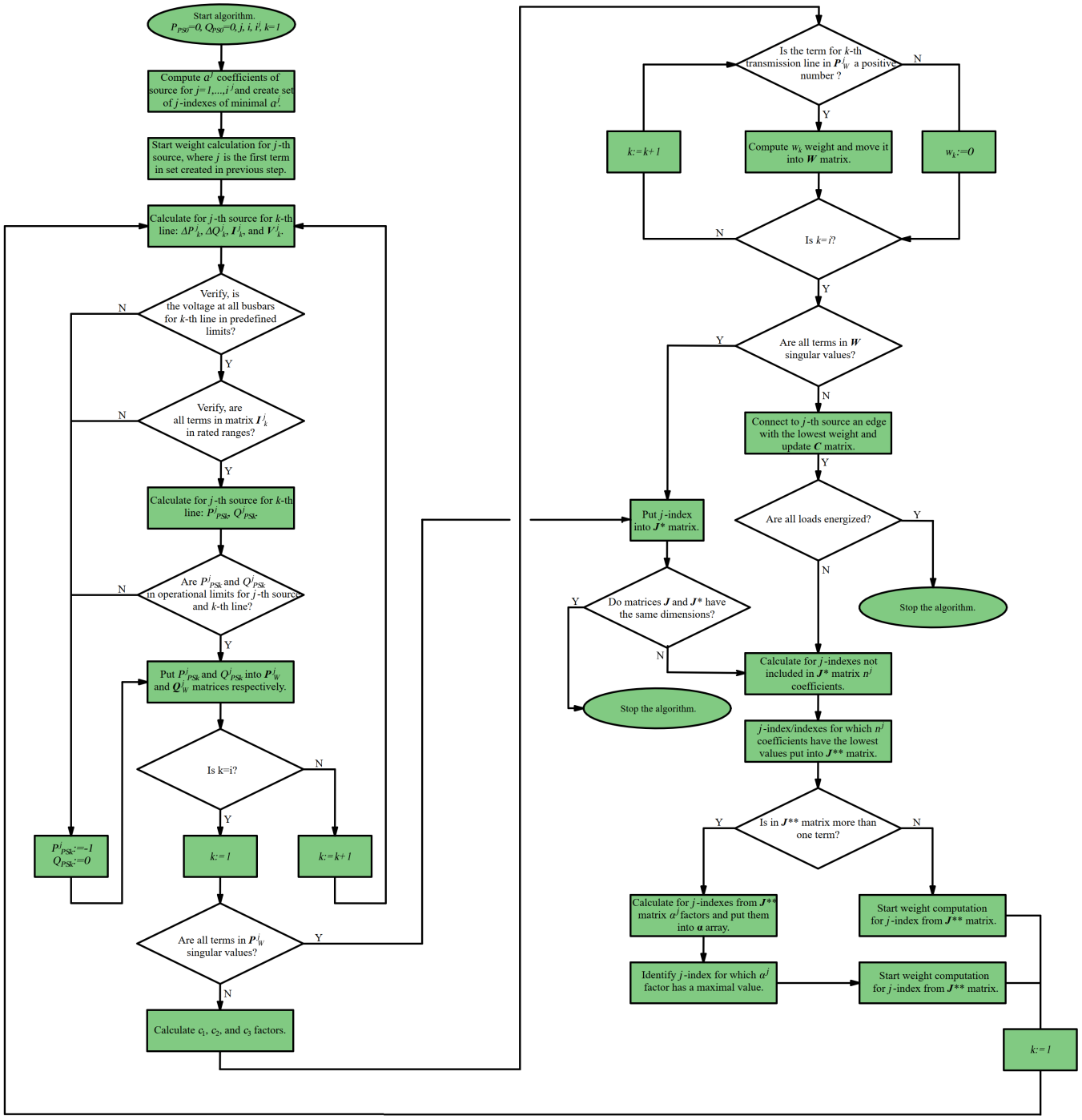

Fig. 8. Algorithm's structure

23. Do matrices $\boldsymbol{J}^*$ and $\boldsymbol{J}$ have the same dimensions?
    (a) If YES, go to step 31.
    (b) If No, go to step 25.
24. Are all loads energized?
    (a) If YES, go to step 31.
    (b) If No, go to step 25.
25. Calculate n^j coefficients given by equation (20) for power sources identified by j-indexes, not present in $\boldsymbol{J}^*$ matrix. The j-indexes for which calculated n^j factor has a minimal value are placed in $\boldsymbol{J}^{**}$ matrix. Then algorithm goes to step 26.
26. Is more than one term in $\boldsymbol{J}^{**}$ matrix?
    (a) If YES, go to step 28.
    (b) If No, go to step 27.
27. Start computation of weight for micro-grid powered by j-th source, where j is a term from $\boldsymbol{J}^{**}$ and go to step 3. Weights are calculated for edges that after connection do not create cycles in topology and do not create energy transfers between micro-grids bounded with each of the energy sources.
28. Calculate set of α^j factors, given by equation (21) for j-indexes included as a term in $\boldsymbol{J}^{**}$ matrix and contain them into array α. Then go to step 29.
29. Find the j-index for which the α^j coefficient is maximal and go to step 30. In the case when there are at least the same two values of α^j factors, j is equal to the first term in $\boldsymbol{J}^{**}$ which fulfills the mentioned condition above.
30. Start computation of the weight for micro-grid powered by j-th source, where j is a term defined in step 29 and go to step 3. Weights are calculated for edges that after connection do not create cycles in topology and do not create energy transfers between micro-grids bounded with each of the energy sources.
31. Stop the algorithm.

The algorithm logic presented in a graphical form is shown in Fig. 8.

5. TEST OF THE ALGORITHM APPLICABILITY

The applicability of the algorithm concept has to be verified in simulations. An object is the core of tests. In this case, it is a power system grid model. Different types of reliability test systems are available in electrical power engineering, i.e., New-England power system, IEEE 14-bus system, IEEE 30-bus system, etc. [30].

These structures include different levels of voltages and their topology is dedicated to verifying power system stability [31]. In the paper [11], authors focused on a test power system dedicated to checking the applicability of their proposed algorithm.

The verification of our novel logic also forces us to create a proper power system grid model. It makes it possible to test the algorithm for multi-sourced power systems, described in the previous part of the paper. Our novel solution is compared with the control logic described in [11].

5.1. Power system test benchmark

The power system benchmark consists of 26 lines and 17 busbars with loads. It operates on a voltage equal to 20 kV. The transmission power losses in transformers are omitted because the main application of the benchmark is a verification of the algorithm described in this paper. The grid configuration is shown in Fig. 9.

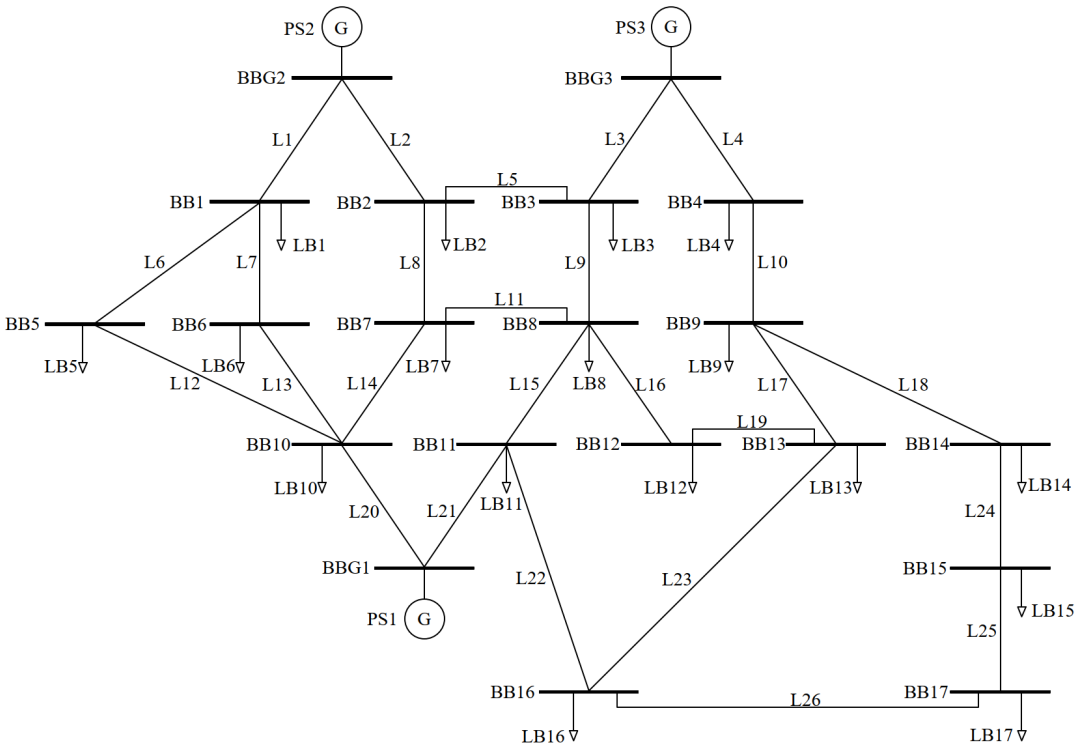

Fig. 9. Power system benchmark topology

The power source capacity is assumed as the same generators. Their rated apparent power is equal to 8 MVA. The test grid aluminum transmission lines are characterized by cross-section, which is equal to 240 mm^2, rated current is equal to 425 A, resistance per unit $R'_L = 0.1292\ \Omega/\text{km}$, reactance per unit $X'_L = 0.1099\ \Omega/\text{km}$ and susceptance per unit $B'_L = 97.3894\ \mu\text{S}/\text{km}$. The values of line lengths and loads are shown in Table 1 and Table 2, respectively.

Table 1
Line lengths in power system model

Line tag	Line length [km]	Line tag	Line length [km]	Line tag	Line length [km]
L1	8	L10	11	L19	8
L2	15	L11	20	L20	14
L3	12	L12	13	L21	6
L4	21	L13	9	L22	17
L5	18	L14	17	L23	7
L6	15	L15	12	L24	11
L7	10	L16	7	L25	14
L8	5	L17	11	L26	10
L9	16	L18	6	–	–

Table 2
Power system model loads

Load tag	Load real power [kW]	Load reactive power [kVar]	Load tag	Load real power [kW]	Load reactive power [kVar]
LB1	0.60	0.20	LB10	1.50	0.60
LB2	0.70	0.40	LB11	1.90	1.20
LB3	2.00	0.80	LB12	0.70	0.30
LB4	2.10	0.90	LB13	0.60	0.30
LB5	0.65	0.50	LB14	0.80	0.50
LB6	0.50	0.30	LB15	0.40	0.20
LB7	3.00	1.90	LB16	0.70	0.40
LB8	0.70	0.40	LB17	0.20	0.10
LB9	0.90	0.30	–	–	–

5.2. Power system test results

In the case of the proposed algorithm, the simulations were conducted for a few sets of p-factors. As mentioned in the introduction of this paper, we also did calculations for the algorithm presented in the publication [11]. The examples of the simulation results are shown in a graphical form in Fig. 10.

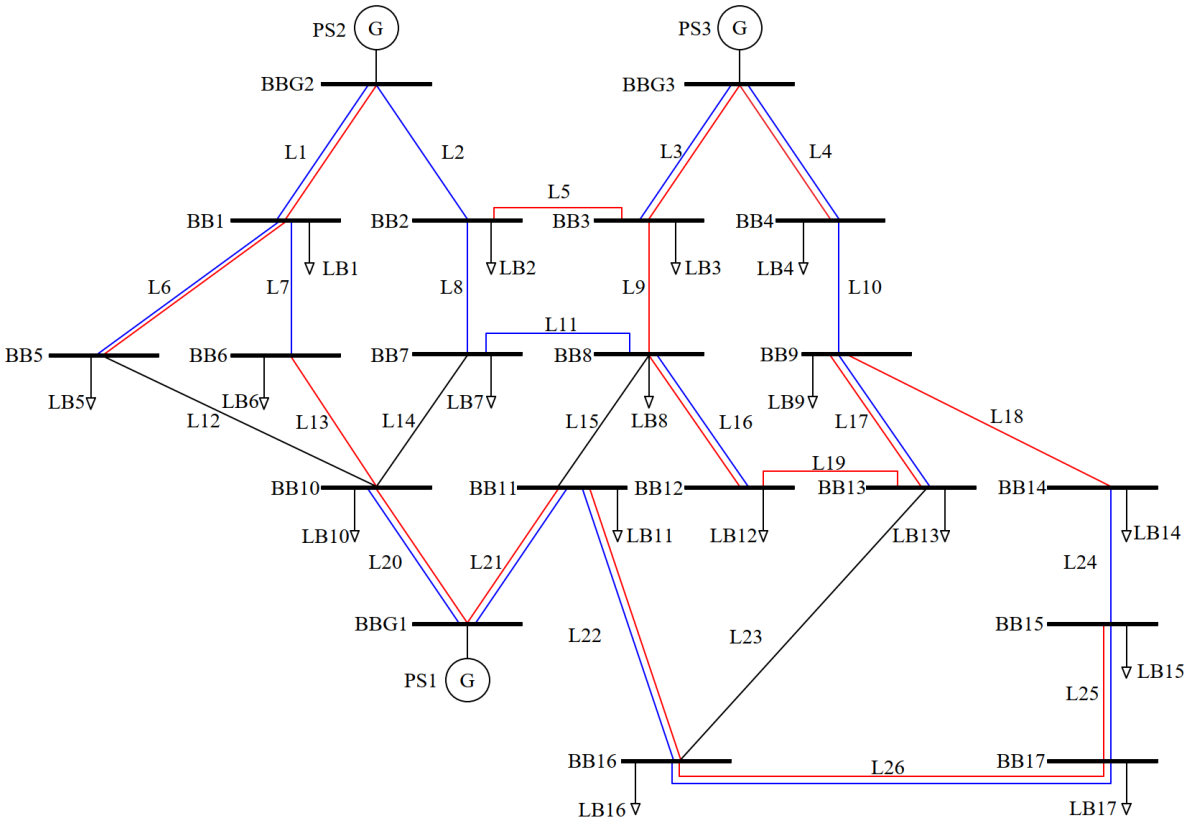

Fig. 10. Simulation results: lines connected as a result of simulations for the algorithm presented in paper [6] (red lines); lines connected asa result of simulations for $p_1 = 1$, $p_2 = 0$, and $p_3 = 0$ (blue lines); lines not connected in any of previously mentioned simulations (blacklines)

The most optimal configuration of *p*-factors, for which all loads are connected and the *MRPL* has the lowest value was verified by PSO. Calculation results are also obtained from more than only the optimal set of *p*-factors and they are presented in a tabular form in Table 3. The table contains the values of S_r, P_r, Q_r, ΔP_r, *MLR*, and *MRLP* which are important for power system topology.

5.3. Discussion

The applicability of the algorithm is verified by specific criterion. In this case two factors have been used: *MLR* and *MRLP*. The main target is to clarify for which set of *p*-coefficients a power system with all loads energized has been created. To minimize real power system losses is equally important. This kind of requirements have a critical influence on the created power grid topology and its exploitation.

For the gathered simulation results in Table 3, the lowest power losses are for the topology when $p_1 = 0$, $p_2 = 0$, and $p_3 = 1$. Those values were defined as optimal by the PSO algorithm. In this kind of situation, the algorithm was considering weights only based on real power losses. The first interpretation of the results may be that the presented algorithm always returns topology with minimal power losses when $p_1 = 0$, $p_2 = 0$, and $p_3 = 0$. This impression may lead to the wrong interpretation of the function of weights in the algorithm. The algorithm adds the line with the lowest weight to the existing spanning tree, but in the end, the final obtained topology may not be the one with the lowest power losses. It is an implication of power flow in a grid and the fact that weights are only calculated locally (for energized nodes, adjacent to the lines not connected now of calculations). The proof is seen for $p_1 = 0$, $p_2 = 0$, and $p_3 = 0$, where the algorithm is focused on reactive power minimization, but the lowest reactive power value, when only cases with all loads energized are considered, is given for $p_1 = 3$, $p_2 = 2$, and $p_3 = 1$.

The weight calculation equation (13) allows one to get different grid topologies. This quality may be called flexibility. The results in Table 3 show that not always all loads are connected to a power source. The final topology is dependent on set p-factors. The wide range of set points which can be defined makes an algorithm more flexible. For example, for $p_1 = 2$, $p_2 = 1$, and $p_3 = 1$ not all loads were powered, but the situation was vastly different for $p_1 = 1$, $p_2 = 1$, and $p_3 = 1$.

The spanning trees creation process is another important advantage of the algorithm. However, the algorithm presented in [11] has a serious defect. The solution may lead to suboptimal behavior shown in Fig. 6. The authors of [11] have pointed to that defect themselves. The solution presented in this paper allowed for the elimination of the previously mentioned weak spot. It was possible by applying equations (20) and (21). A comparison of the results obtained by the algorithm from [11] and the novel logic from this paper proves the utility of the proposed solution. In the first case, not all loads are connected, and finally, only about 85% of the requested power is delivered to the receivers. When the algorithm is also only based on calculated weights The second case gives a completely different result for the real power. *MLR* factor is equal to 1, and all loads are energized.

Table 3
Simulation results

The algorithm presented in the paper			S_r [MVA]	P_r [MW]	Q_r [MVar]	ΔP_r [MW]	*MLR*	*MRLP*	*t* [ms]
p_1	p_2	p_3							
1.00	1.00	1.00	18.24	18.24	0.14	0.34	1.00	0.34	299
2.00	1.00	1.00	15.26	15.21	–1.23	0.31	0.83	0.37	297
1.00	2.00	1.00	18.24	18.24	0.14	0.34	1.00	0.34	315
1.00	1.00	2.00	18.24	18.24	0.14	0.34	1.00	0.34	350
1.00	2.00	3.00	18.27	18.27	0.46	0.37	1.00	0.37	322
1.00	3.00	2.00	18.27	18.27	0.46	0.37	1.00	0.37	317
2.00	1.00	3.00	18.30	18.29	0.46	0.40	1.00	0.40	344
3.00	1.00	2.00	18.27	18.27	0.46	0.37	1.00	0.37	330
2.00	3.00	1.00	18.27	18.27	0.46	0.37	1.00	0.37	341
3.00	2.00	1.00	18.40	18.40	0.05	0.50	1.00	0.50	315
1.00	0.00	0.00	18.27	18.26	0.33	0.36	1.00	0.36	297
0.00	1.00	0.00	18.24	18.24	0.14	0.34	1.00	0.30	313
0.00	0.00	1.00	18.21	18.20	0.60	0.30	1.00	0.30	339
The algorithm from the paper [6]			15.29	15.23	–1.34	0.28	0.85	0.33	316

The efficiency of simulation for the presented algorithm could be measured as the time needed to complete the logic in Fig. 6. However, this kind of analysis is not a subject of this paper because it depends on the number of edges for which weights are calculated. Each set of *p*-factors influences the time needed by the algorithm. For example, in the first step, the weights are calculated only for two lines whereas in the next step it is done for six lines. In this case, the time of the second step is almost three times longer than for the first step. This situation excludes the treatment of the simulation time as the representative datum. The time of each of the simulations did not exceed 350 ms.

6. CONCLUSIONS

The development of Smart Grid technologies requires algorithms used in restoration strategies. The logic presented in this paper belongs to this group. The described algorithm is fully applicable and may serve as an alternative for solutions based on the graph sectionalizing methodology.

A simplified algorithm structure is a definite advantage in the proposed solution. The sectionalizing method splits grid topology into smaller parts and calculates weights that are used to create micro-grids. As a result, for each source topology of the transmission line spanning trees is built. The algorithm described in the paper gives an alternative possibility. Spanning trees are created from the beginning, bounded with each of the power sources in the analyzed grid. The main contribution of this article is a formulation of the conditions, which eliminate a suboptimal Prim's algorithm behavior in the context of multi-sourced power systems, e.g., insufficient power balance between energy generators [11]. It guarantees the proper switching between sources for a greedy algorithm connecting transmission lines and loads. Simulations must be verified, and this advantage must be confirmed. The novel algorithm was better than already existing solutions represented by the reference logic described in [11] because it returns as a result structure with all loads connected. The computation affords of the reference algorithm and the new one may be considered as the same. The average simulation time presented in this paper logic is equal to about 321 ms and the reference one needed 316 ms to complete all necessary computations.

Graph theory algorithms are based on weights. The described novel multi-parametrized weight calculation formula offers wider possibilities than those using only a single variable, e.g., real power. It is especially crucial for a grid when it is not possible to connect all loads to a local power system. From an economical point of view in such a case, it is expected to energize loads, which require higher electrical power values. The simulation results prove that the proposed weight calculation method is better than the idea of using weights based only on a single parameter. The reference algorithm using weights calculated on real power in [11] does not energize all loads in a considered simulation topology. Equation (13) applied in the algorithm proposed in this paper guaranteed power delivery to all recipients.

The discussed algorithm still leaves some problems connected with weights calculations unsolved. The multi-parametrized formula requires the setting of *p*-factors. Particle swarm optimization may define them for quality factors, e.g., minimization of power losses. This problem needs some further analysis.

REFERENCES

[1] S.A. Arefifar, Y.A.-R.I. Mohamed, and T.H.M. EL-Fouly, "Comprehensive Operational Planning Framework for Self-Healing Control Actions in Smart Distribution Grids," *IEEE Trans. Power Syst.*, vol. 28, no. 4, pp. 4192–4200, 2013, doi: 10.1109/tpwrs.2013.2259852.

[2] J. Quiros-Tortos and V. Terzija, "A Graph Theory Based New Approach for Power System Restoration," in Proc. *2013 IEEE Grenoble PowerTech (POWERTECH)*, 2013, doi: 10.1109/ptc.2013.6652108.

[3] T.D. Sudhakar and K.N. Srinivs, "Power System Reconfiguration Based on Prim's Algorithm," in Proc. *2011 1st International Conference on Electrical Energy Systems (ICEES)*, 2011, doi: 10.1109/ICEES.2011.5725295.

[4] M.M. Ibrahim, H.A. Mostafa, M.M.A. Salama, R. El-Shatshat, and K.B. Shaban, "A Graph-theoretic Service Restoration Algorithm for Power Dystribution Systems," in Proc. *2018 International Conference on Innovative Trends in Computer Engineering (ITCE)*, 2018, doi: 10.1109/itce.2018.8316647.

[5] A. Golshani, W. Sun, and K. Sun, "Advanced power system partitioning method for fast and reliable restoration: toward a self-healing grid," *IET Gener. Transmiss. Distrib.*, vol. 12, no,1, pp.45–52, 2018, doi: 10.1049/iet-gtd.2016.1797.

[6] J. Quiros-Tortos, M. Panteli, P. Wall, and V. Tereija, "Sectionalising methodology for paraller system restoration based on graph theory," *IET Gener. Transmiss. Distrib.*, vol. 9, no. 11, pp. 1216–1225, 2015, doi: 10.1049/iet-gtd.2014.0727.

[7] M. Parol, P. Kapler, J. Marzecki, R. Parol, M. Połecki, and Ł. Rokitnicki, "Effective approach to distributed optimal operation control in rural low voltage microgrids," *Bull. Pol. Acad. Sci. Tech. Sci*, vol. 68, no. 4, pp. 661–678, 2020, doi: 10.24425/bpasts.2020.134178.

[8] S. Sannigrahi, S.R. Ghatak, and P. Acharjee, "Multi-objective optimisation-based active distribution system planning with reconfiguration, intermittent RES and DSTATCOM," IET Renew. Power Gener., vol. 13, no. 13, pp. 2418–2429, 2019, doi: 10.1049/iet-rpg.2018.6060.

[9] A. Bonfilio, M. Invernizzi, A. Labella, and R. Procopio, "Design and Implementation of a Variable Synthetic Inertia Controller for Wind Turbine Generators," *IEEE Trans. Power Syst.*, vol. 34, no. 1, pp. 754–764, 2019, doi: 10.1109/tpwrs.2018.2865958.

[10] F. Vazinram, R. Effatnejad, M. Hedayati, and P. Hajihosseini, "Decentralised self-healing model for gas and electricity distribution network," *IET Gener. Transmiss. Distrib.*, vol. 13, no. 19, pp. 4451–4463, October 2019, doi: 10.1049/iet-gtd.2019.0416.

[11] M. Eriksson, M. Armendariz, O. Vasilenko, A. Saleem, and L. Nordström, "Multi-Agent Based Distribution Automation Solution for Self-Healing Grids," *IEEE Trans. Ind. Electron.*, vol. 62, no. 4, pp. 2620–2628, 2015, doi: 10.1109/tie.2014.2387098.

[12] J. Li, *Reconfiguration of power network based on graph-theoretic algorithms*, Graduate Theses and Dissertations, Iowa State University, 2010, pp. 10–35, doi: 10.31274/etd-180810-2753.

[13] T.H. Cormen, C.E. Leiserson, R.L. Rivest, and C. Stein, "Section 23.2: The algorithms of Kruscal and Prim" in *Introduction to Algorithms*, 3rd ed., MIT Press, 2009, pp. 631–638.

[14] J. Ansari, A. Gholami, and A. Kazemi, "Multi-agent systems for reactive power control in smart grids," *Int. J. Electr. Power Energy Syst.*, vol. 83, pp. 411–425, 2016, doi: 10.1016/j.ijepes.2016.04.010.

[15] M. Borecki, M. Ciuba, Y. Kharchenko, and Y. Khanas, "Substation reliability evaluation in the context of the stability prediction of power grids," *Bull. Pol. Acad. Sci. Tech. Sci*, vol. 68, no. 4, pp. 769–776, 2020, doi: 10.24425/bpasts.2020.134170.

[16] Q. Wang, S. Tao, X. Du, C. Zhong, and Y. Tang, "Coordinating Control Strategy for Multi Micro Energy Systems Within Distribution Grid Considering Dynamic Characteristics and Contradictory Interests," *IEEE Access*, vol. 7, pp. 139548–139559, 2019, doi: 10.1109/access.2019.2943926.

[17] Z. Wang and J. Wang, "Self-healing resilient distribution systems based on sectionalization into microgrids," *IEEE Trans. Power Syst.*, vol. 30, no. 6, pp. 3139–3149, 2015, doi: 10.1109/tpwrs.2015.2389753.

[18] W. Bąchorek and M. Benesz, "Analysis of sectionizing switch placement in medium voltage distribution networks in the aspect of improving the continuity of power supply," *Bull. Pol. Acad. Sci. Tech. Sci*, vol. 68, no. 3, pp. 459–466, 2020, doi: 10.24425/bpasts.2020.133377.

[19] R.J. Wilson, *Introduction to Graph Theory*, London, Pearson Education Limited, 2010, pp. 8–79.

[20] J.A. Bondy and U.S.R. Murty, *Graph theory with applications*. London, Citeseer, 1976, pp. 10–55.

[21] B.S. Torres, L.R. Ferreira, and A.R. Aoki, "Distributed Intelligent System for Self-Healing in Smart Grids," *IEEE Trans. Power Del.*, vol. 33, no. 5, pp. 2394–2403, 2018, doi: 10.1109/tpwrd.2018.2845695.

[22] X. Yang, Y. Zhang, H. He, S. Ren, and G. Weng, "Real-Time Demand Side Management for a Microgrid Considering Uncertainties," *IEEE Trans. Smart Grid*, vol. 10, no. 3, pp. 3401–3414, 2019, doi: 10.1109/tsg.2018.2825388.

[23] A. Younesi, H. Shayeghi, A. Safari, and P. Siano, "Assessing the resilience of multi microgrid based widespread power systems against natural disasters using Monte Carlo Simulation," *Energy*, vol. 207, 118220, 2020, doi: 10.1016/j.energy.2020.118220.

[24] Y. Shen, Y. Chen, J. Zhang, Z. Sang, and Q. Zhou, "Self-Healing Evaluation of Smart Distribution Network Based on Uncertainty Theory," *IEEE Access*, vol. 7, pp. 140022–140029, 2019, doi: 10.1109/access.2019.2939537.

[25] K. Anoh, S. Maharjan, A. Ikpehai, Y. Zhang, and B. Adebisi, "Energy Peer-to-Peer Trading in Virtual Microgrids in Smart Grids: A Game-Theoretic Approach," *IEEE Trans. Smart Grid*, vol. 11, no. 2, pp. 1264–1275, 2020, doi: 10.1109/tsg.2019.2934830.

[26] A. Chris and V. Koivunen, "Coalitional Game-Based Cost Optimalization of Energy Portfolio in Smart Grid Communities," *IEEE Trans. Smart Grid*, vol. 10, no. 2, pp. 1960–1970, 2019, doi: 10.1109/TSG.2017.2784902.

[27] M. Zadsar, M.R. Haghifam, and S.M.M. Larimi, "Approach for self-healing resilient operation of active distribution network with microgrid," *IET Gener. Transmiss. Distrib.*, vol. 11, no. 18, pp. 4633–4643, 2017, doi: 10.1049/iet-gtd.2016.1783.

[28] W. Jiang, C. Yang, Z. Liu, M. Liang, P. Li, and G. Zhou, "A Hierarchical Control Structure of Distributed Energy Storage System in DC Micro-Grid," *IEEE Access*, vol. 7, pp. 128787–128795, 2019, doi: 10.1109/access.2019.2939626.

[29] K. Karimizadeh, S. Soleymani, and F. Faghihi, "Optimal placement of DG units for the enhancement of MG networks performance using coalition game theory," *IET Gener. Transmiss. Distrib.*, vol. 14, no. 5, pp. 853–862, 2020, doi: 10.1049/iet-gtd.2019.0070.

[30] J. Machowski, J. W. Bialek, and J. R. Bumby, *Power System Dynamics: Stabilty and Control*. Haboken, New Jersey, John Wiley & Sons, Ltd., 2008, pp. 89–99.

[31] P. Li, J. Ji, H. Ji, G. Song, Ch. Wang, and J. Wu, "Self-healing oriented supply restoration method based on the coordination of multiple SOPs in active distribution networks," *Energy*, vol. 195, 116968, 2020, doi: 10.1016/j.energy.2020.116968.

[32] S. Pochpor and H.M. Suryawanshi, "Design and Analysis of Triplen Controlled Resonant Converter for Renewable Sources to Interface DC Micro Grid," *IEEE Access*, vol. 7, pp. 15330–15339, 2019, doi: 10.1109/access.2019.2891165.

[33] S. Heinen and M.J. O'Malley, "Complementarities of Supply and Demand Sides in Integrated Energy Systems," *IEEE Trans. Smart Grid*, vol. 10, no. 1, pp. 1156–1165, 2019, doi: 10.1109/tsg.2018.2871393.

[34] F. Liberati, A. Di Giorgio, A. Giuseppi, A. Pietrabissa, E. Habib, and L. Martirano, "Joint Model Predictive Control of Electric and Heating Resources in a Smart Building," *IEEE Trans. Ind. Electron*, vol. 55, no. 6, pp. 7015–7027, 2019, doi: 10.1109/TIA.2019.2932954.

[35] A. Mojallal, S. Lotfifard, and S.M. Azimi, "A Nonlinear Supplementary Controller for Transient Response Improvement of Distributed Generations in Micro-Grids," *IEEE Trans. Sustain. Energy*, vol. 11, no. 1, pp. 489–499, 2020, doi: 10.1109/tste.2019.2895961.

[36] S. Gude and Ch-Ch Chu, "Single Phase Enhanced Phase-Locked Loops Based on Multiple Delayed Signal Cancellation Filters for Micro-Grid Applications," *IEEE Trans. Ind. Electron*, vol. 55, no. 6, pp. 7122–7133, 2019, doi: 10.1109/TIA.2019.2915563.